River Flow 2010 - Dittrich, Koll, Aberle & Geisenhainer (eds) - © 2010 Bundesanstalt für Wasserbau ISBN 978-3-939230-00-7

Incipient rolling of coarse particles in water flows: a dynamical perspective

M. Valyrakis, P. Diplas & A. O. Celik
Department of Civil and Environmental Engineering, Virginia Tech, Blacksburg, VA, USA

C. L. Dancey
Department of Mechanical Engineering, Virginia Tech, Blacksburg, VA, USA

ABSTRACT: Understanding the processes that trigger the onset of motion and entrainment of coarse bed material is one of the fundamental problems in earth-surface dynamics. The objective of this paper is to analytically formulate and experimentally validate a criterion for the entrainment of exposed grains by rolling, due to the action of fluctuating hydrodynamic forces. Here, the rapidly varying turbulent forces are modeled as pulses of specific duration and magnitude. The momentum balance equations are implemented to derive the critical force above which the momentum transfer to the grain is positive, while the grain dislodges. Appropriately designed experiments are performed in a tilted flume, to investigate the incipient motion of an individual spherical particle. Statistical analysis of the parameters characterizing grain entrainment and trajectory analysis of typical entrainment events is offered. The experimentally obtained data are compared with the theoretical results. It is concluded that only the sufficiently persisting, high magnitude pulses may result in grain entrainment.

Keywords: Grain entrainement, Impulse, Turbulence

1 INTRODUCTION

1.1 *Traditional approaches to grain entrainment*

The interaction of turbulent fluid flow with its solid boundary, results in soil erosion in rivers and estuaries which constitutes a central problem in engineering and earth surface dynamics (Syvitski et al. 2005). Of particular interest to the fields of civil and environmental engineering and stream ecology is the identification of threshold flow conditions which are critical to the mobilization of coarse sedimentary grains. Typical applications range from the protection of hydraulic structures from scouring processes to the selection of minimum grain sizes for channel bed stabilization. In the case of contaminated bed material, accurate assessment of the flow conditions leading to removal and downstream transport to sites of ecological or other significance (e.g. water supply intakes) is vital. Such information is also substantial for establishing the maximum flushing flow conditions downstream reservoirs, while avoiding transport rates that may be damaging to stream's ecology and spawning habitats.

Much of the bedload transport, especially at low transport stages, occurs by rolling. Over the past decades the initiation of grain mobilization by rolling has been investigated under a theoretical deterministic framework (White 1940, Coleman 1967, Komar & Li 1988, James 1990, Ling 1995). Most of these studies assume the influence of various hydrodynamic and resisting forces, acting on an exposed to the incident flow grain, which rests on top of a local bed arrangement. According to the traditional static equilibrium approach, grain mobilization is dictated from the balance of moments about a rolling axis.

The spatiotemporal variability of both flow forcing as well as micro-topography parameters can be incorporated employing a probabilistic approach (Kirchner et al. 1990, Papanicolaou et al. 2002, Wu & Chou 2003, Hofland & Battjes 2006). Distributions of parameters related to local bed geometry and grain arrangement, such as particle's exposure (Paintal 1971a, Hofland et al. 2005) or relative protrusion (Fenton & Abbott 1977, Chin & Chiew 1993) and relative flow depth (Shvidchenko & Pender 2000) can be found in the literature.

1.2 *Grain entrainment from a dynamical perspective*

The significance of fluctuating local velocity and pressure field on the transport of bed material has been emphasized in the literature (Zanke 2003, Sumer et al. 2003, Hofland et al. 2005, Schmeeckle et al. 2007, Vollmer & Kleinhans 2007).

However, the complete entrainment and trajectory of individual coarse particles greatly depends on the time history of hydrodynamic forcing (McEwan & Held 2001, Schmeeckle & Nelson 2003, Valyrakis et al. 2008, Yeganeh-Bakhtiary et al. 2009). Diplas et al. (2008), was the first to present a dynamical framework for the entrainment of particles, based on the impulse (I_i) criterion. According to this concept, impulse is defined as the product of the hydrodynamic force ($F(t)$), with the duration (T_i) for which the critical force (F_{cr}) is exceeded:

$$I_i = \int_{t_i}^{t_i+T_i} F(t)dt, \text{ for } F(t) > F_{cr} \quad (1)$$

Valyrakis et al. (in press) extended the theoretical analysis and experimental results to illustrate the effect of duration of energetic events in addition to the magnitude of the fluctuating hydrodynamic forces. The critical flow impulse events were modeled as idealized square pulses responsible for transmitting enough momentum for the full entrainment of the grain. Critical levels of impulsive force and duration where derived, for variable local bed configurations and degrees of entrainment of saltating or rolling grains. Thus flow events with relatively high impulse content which occur sporadically can cause the complete entrainment of spherical particles out of their resting configuration. On the contrary and consistent with lab observations, if the flow strength does not last for a sufficient amount of time the grain may not complete its entrainment downstream and will fall back to its initial location.

Closer investigation of experimental data on the displacement of individual grains reveals the possibility that dislodgement is caused from a sequence of impulses rather than a single impulse event. Such impulses are below critical and would not suffice to cause complete grain dislodgement if they were isolated. To further investigate the above observation, the dynamics of grain entrainment are appropriately analyzed. For that reason, grain trajectories and the distributions of quantities that statistically characterize the phenomenon are discussed. The impulse theory is extended to include the effect of varying resisting forces as the grain is dislodged. Experimentally obtained results are offered to support the proposed hypothesis.

2 THEORETICAL ANALYSIS

2.1 *Grain entrainment by rolling*

Incipient movement of a spherical particle, exposed to the flow occurs by rolling when the following conditions are satisfied:

$$\Sigma F_\theta = F_D \sin(\theta_0 - \alpha) + B_f \cos(\theta_0 - \alpha) - W \cos\theta_0 > 0 \quad (2a)$$

$$\Sigma F_\xi = -F_D \cos(\theta_0 - \alpha) + B_f \sin(\theta_0 - \alpha) - W \sin\theta_0 < 0 \quad (2b)$$

where the gravitational (W), buoyancy (B_f) and drag (F_D) are considered to act on the center of mass of the grain, θ_0, is the pivoting angle, formed between the horizontal and the lever arm (L_{arm}), ΣF_ξ , ΣF_θ represent the sum of forces in the radial, ξ, and tangential, θ, directions at the rest position, respectively (Figure 1). Equation (2a) implies that the grain accelerates in the tangential direction while Equation (2b), is required for the particle to maintain contact with the downstream particles as it rolls out of its resting pocket.

Valyrakis et al. (2010), employed the equations of motion for a rolling grain, to derive the minimum required duration (T) for an application of hydrodynamic forcing above critical ($F_D > F_{cr}$ or $\Sigma F_\theta > 0$), which results in its complete dislodgement downstream:

$$T = \sqrt{\frac{L_{arm} m_{\text{mod}}}{-\Sigma F_\xi}} \operatorname{arcsinh}\left(\sqrt{2W\rho_\theta} \frac{\sqrt{-\Sigma F_\xi}}{\Sigma F_\theta} \right) \quad (3)$$

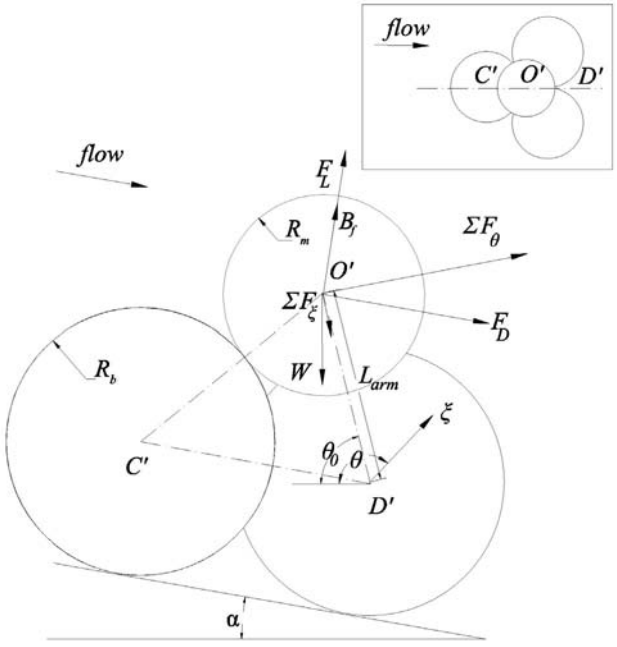

Figure 1. . Definition sketch of tetrahedral particle arrangement for entrainment by rolling, due to application of drag (F_D) force of certain duration (T).

where $m_{mod} = (7/5\ \rho_s + \rho_f\ C_m)V$, is an expression for the mass of the particle accounting for added mass effects, ρ_f and ρ_s are the fluid and solid densities, V, is the particle's volume, C_m, is the added mass coefficient and ρ_θ, is a geometrical coefficient depending on the ratio of exposed to base solid grains:

$$\rho_\theta = \lambda(1-\sin\theta_0)\left(\frac{\cos\theta_0}{1-\sin\theta_0}\sin\alpha + (\cos\alpha - \frac{\rho_f}{\rho_s})\right) \qquad (4)$$

with λ, the ratio of partial angular dislodgement (θ_{fin}) to the angular displacement for complete entrainment ($\theta_{max}=\pi/2$):

$$\lambda = \frac{\sin(\theta_{fin}) - \sin(\theta_0)}{\sin(\frac{\pi}{2}) - \sin(\theta_0)} \qquad (5)$$

According to equation (5), λ, ranges from 0 for no movement to 1 for complete entrainment. Intermediate values characterize different mobility levels from vibrations to twitches.

2.2 *Concept of sequence of pulses*

The above theory models the rapidly fluctuating turbulent forces as square pulses of specific duration and magnitude. Considering the very small time scales of turbulent fluctuations (of the order of tens of milliseconds to seconds - depending on the size of the grain) which are effective in grain removal, the impulse model is physically sound.

Video observations of particle dislodgement in water flows, reveals cases when the grain performs incomplete displacement or is dislodged relatively slowly to the crest formed by the downstream particles, to be eventually entrained. Based on these observations the impulse model is further extended to include the cumulative effect of secondary impulses. It is hypothesized that a series of impulses occurring at short (relative to their duration) temporal intervals, may act synergistically in completely dislodging a grain by rolling.

As an illustrative example a sequence of two impulses may be considered (Figure 2). Assume for simplicity that the duration of application of all impulses is T. Equation (3) predicts the required force $F_1(> F_{cr})$, for complete grain removal (λ=1) when only a single impulse is applied ($I_1=F_1 T=I_{cr}$, Figure 2a). Applying an impulse I_2 of magnitude F_2, with $F_1> F_2> F_{cr}$, will only result in incomplete displacement ($\theta_{fin}<\pi/2$ or $\lambda<1$). The displacement may be completed if a second impulse (I_3) of magnitude $F_3>F_{cr}'$, follows. Here, F_{cr}', defines the sum of resisting forces which depends on the new angular position the particle has obtained ($\theta(t)<\theta_{fin}$). Figure 2b illustrates the concept based on which the first impulse partially dislodges the

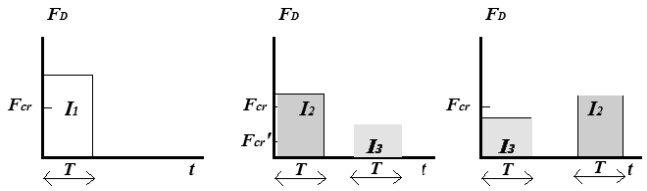

Figure 2. Impulse model generalization: a) single impulse application capable for complete entrainment, b) series of impulses leading to full dislodgement and c) same series of impulses insufficient for complete dislodgement.

grain to a new position where secondary impulses become effective in further pushing the grain, due to reduced resisting forces. In the case the secondary impulse (I_3) arrives before the primary impulse (I_2) or before the grain dislodges to a new position, it is rendered ineffective (Figure 2c).

Thus the impulse model (Equation 3) predicting complete dislodgement for impulses equal or greater to I_{cr}, may be generalized to the sequence of impulses (I_i) formulation:

$$\sum_{i=1}^{n} I_i \geq I_{cr}, \text{ for i=1,2,...,n} \qquad (6)$$

where the flow event i, is ineffective (I_i=0), if it is applied at instances when its strength is less than the corresponding resisting force ($F_i<F_{cr,i}$).

Essentially the required impulse is predicted from the same equation (Eq. 3) as before, with the only difference that a series of flow events are responsible in imparting small positive changes to the particle momentum, until its full removal.

3 EXPERIMENTAL PROCEDURE

Flume experiments are performed to obtain coupled data for the entrainment of a fully exposed Teflon® (specific gravity = 2.3) spherical particle in addition to the flow events causing it. The properties of the near threshold (about 2 entrainments per minute) uniform open channel flow are shown in Table 1. The sphere (12.7mm diameter) rests on top of four layers of fully packed 8mm glass beads, forming a tetrahedral arrangement (Figure 3). The motion of the grain is recorded via a photomultiplier tube (PMT) and a He-Ne laser source. As seen in Figure 3, the He-Ne laser beam is aligned to

Table 1. Time averaged flow properties

U(z) mean	(m/sec)	0.178
U(z) standard deviation	(m/sec)	0.047
U(z) skewness	(m/sec)	0.052
U_* shear velocity	(m/sec)	0.025
Mean entrainment rate	(entr./sec)	0.042
H_{flow} mean flow height	(m)	0.072
Re	(-)	13261
Re_*	(-)	1863

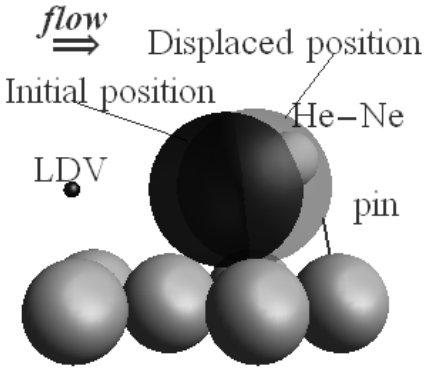

Figure 3. Local particle configuration, showing the uppermost layer of (8mm) glass beads, the LDV measurement volume, the He-Ne beam and the initial and displaced positions of the fully exposed sphere.

partially target the test particle. Its angular dislodgement is a linear function of the signal intensity of the PMT, which changes proportional to the light received by the He-Ne laser beam. A continuous series of entrainments is made possible due to a restraining pin (Figure 3), which limits the maximum dislodgement of the grain to the displaced position. The grain will fall back to its initial position after the energetic flow structure has passed. The time history of the streamwise velocity component one diameter upstream of the particle ($u(t)$) is obtained by means of laser Doppler velocimetry (4W Argon ion LDV) at an average sampling frequency of about 300Hz. Utilizing Equation (1), the impulse events can be extracted from the time series of F_D=f(u^2), considering the classical drag formulation. The 30 minutes long, synchronized time series of impulses and streamwise grain displacement are statistically analyzed and the detailed trajectory analysis during the dislodgement events is offered.

4 RESULTS

4.1 *Statistical analysis*

The entrainment of coarse sediment particles at near incipient flow conditions is a highly dynamic and intermittent process. Due to the variability of the flow field only a probabilistic description of the phenomenon is feasible, even for an individual grain resting on a fixed local bed arrangement (Papanicolaou et al. 2002). Consecutively, for the proper statistical description of characteristic parameters, histograms of their probability distribution are provided.

In Figure 4a, the distribution of time over which the grain remains suspended due to flow events of sufficient energy is shown. This duration is indicative of the temporal distance between positive and negative peaks in the flow. The former are required for onset of entrainment, while the later for distrainment of the completely exposed grain. As such this measure corresponds to the time scale of the macroscale turbulent flow structures typically having length of several flow depths. The distribution of durations required for a complete dislodgement event is illustrated in Figure 4b. The duration for dislodgement, is generally inversely proportional to the mean angular velocity (Fig. 4c) or change momentum of the grain and can be considered as indication of the magnitude of the offered flow impulses. The distributions of those parameters are in qualitative agreement with corresponding measurements reported in the literature (Drake et al. 1988, Williams 1990).

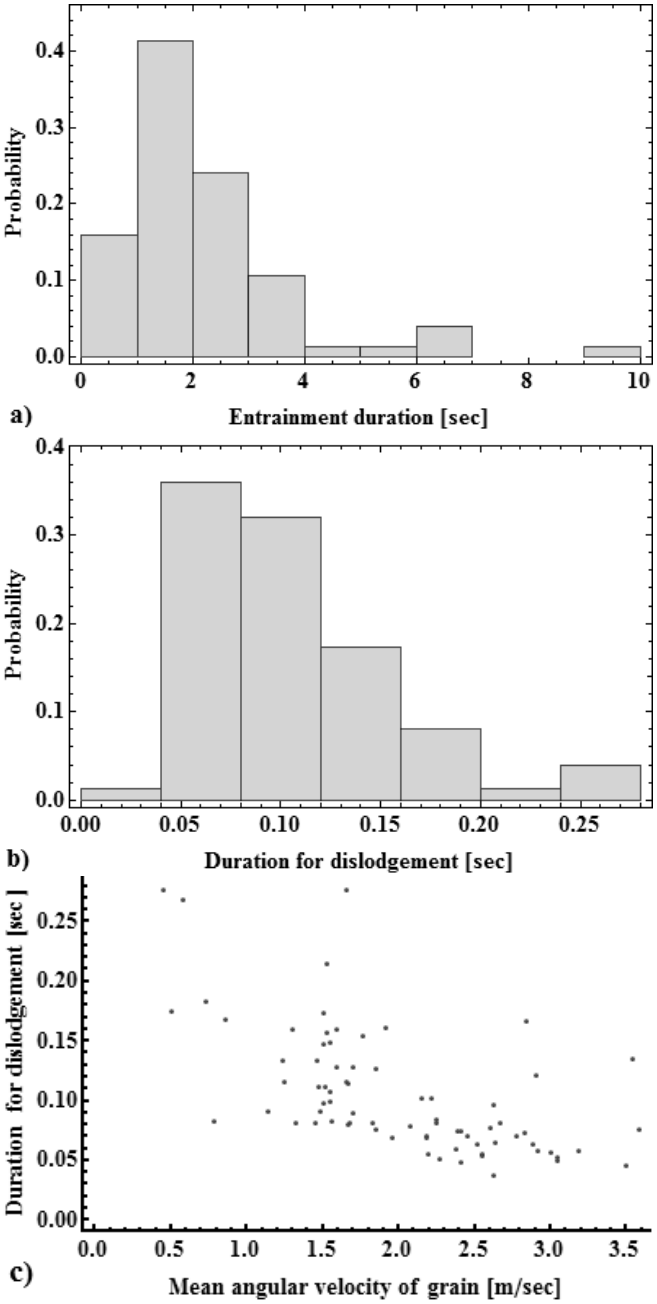

Figure 4. a) probability distribution of entrainment durations, b) probability distribution of durations for complete dislodgement, and c) scatter plot of the average angular velocities with duration for dislodgement for all grain entrainment events.

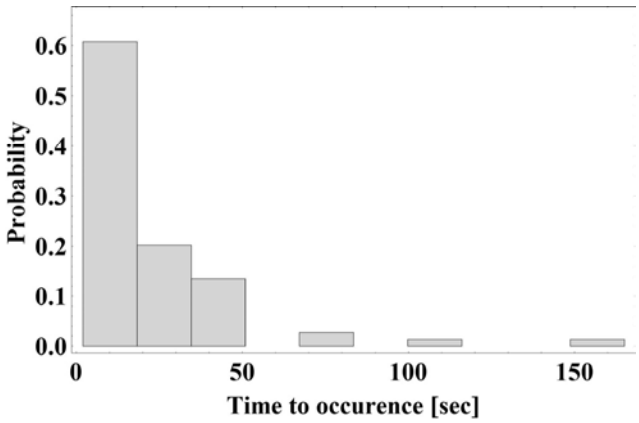

Figure 5. Distribution of time to occurrence of entrainment events.

4.2 *Reliability of grain dislodgement*

The traditional statistical analysis may be complemented utilizing reliability theory or survival analysis. Under this framework, the entrainment of an individual coarse grain may be regarded as a stochastic process with a certain probability that the grain will "survive" the entrainment for a specific time interval. Similar concepts have been employed from Ancey et al. (2007) who considered the flux of coarse grains as a birth-death process as well as Tucker & Bradley (2009) for sediment motion along a transport path.

Reliability theory usually models the rate of occurrences or time interval until the event investigated takes place. Here of interest is the complete entrainment of the individual test particle. The probability distribution of time to occurrence (recurrence intervals) of entrainment events is shown in Figure 5. The distribution of intervals between occurrences of entrainment (Fig. 4c), shows high kurtosis which is indicative of high intermittency. The mean of inter-arrival times between dislodgement events is a commonly measured reliability parameter and may be found as the inverse of the entrainment rate (Table 1), having a value of 24 sec.

Nonparametric analysis of the entrainment instances is performed, employing the Kaplan-Meier estimator (Kaplan & Meier 1958):

$$R(t_i) = \prod_{j=1}^{i} \frac{n_j - k_j}{n_j}, \text{ for } i = 1,2,...,m \tag{7}$$

where t_i is the duration interval over which the particle is expected to dislodge, n_i is the number of dislodgements expected to occur after time t_i-1, k_i is the number of dislodgements occurring during t_i, and m is the total number of entrainment events. The obtained values provide an estimation of the reliability that a grain will not have been entrained over a particular duration interval (Figure 6). For example, the mean interval between entrainments (24 sec), is given by R=0.5.

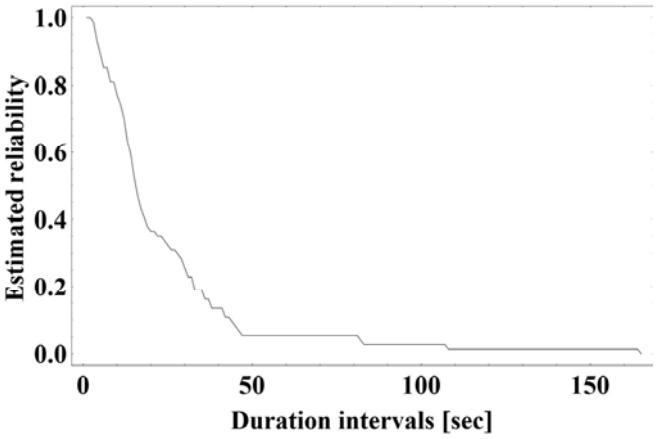

Figure 6. Plot of Kaplan-Meier estimator as a measure of nonparametric reliability.

4.3 *Comparison of experimental data to theoretical predictions*

The distribution of grain angular velocities averaged over the duration for dislodgement relates to the distribution of impulses or sequence of impulses which are effective in completely displacing it. In the following, all impulse events are offered to enable comparison to the theoretical results.

Utilizing the time series of instantaneous velocity signal upstream the particle the potentially effective impulses are acquired from Equation 1. These are grouped together to separate flow events, if their temporal distance does not exceed a defined duration, which is typically selected to be less than the average duration for dislodgement. Then the impulses belonging to the same flow event are summed according to Equation 6, so that their combined effect can be accounted for.

Figure 7, offers a comparison of the experimentally obtained results with the theoretical curves as predicted from Equation 3. Impulse events are extracted using the simplifying assumption of constant F_{cr} (corresponding to constant critical velocity level with drag coefficient of C_D=1). The flow events above the threshold curve (C_D=1, Figure 7), will result in complete entrainment of the test particle, while the points below the curve will only produce small vibrations to twitches depending on their proximity to the critical curve.

The impulse content of the flow events is illustrated in Figure 8. It is important to note that for the flow events of variable duration and magnitude, the theoretical curves remain practically constant. For example the threshold curve, for C_D=1, appears to undergo a change of less than 10%, for the range of flow events of interest. The

relative invariability of impulse (compared to the more than twofold variation of the magnitude of flow events, for the same range of values), is indicative of the potential usefulness of impulse as a criterion for grain entrainment.

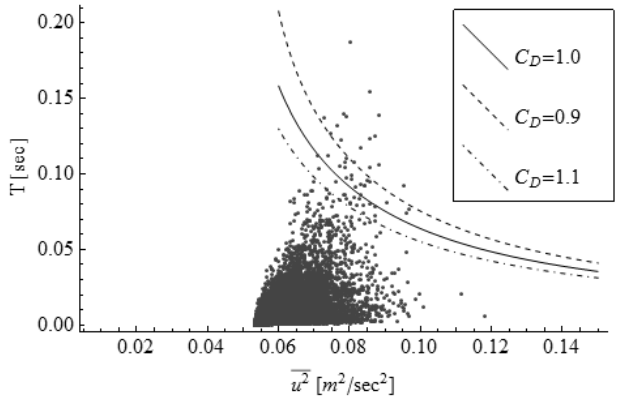

Figure 7. Magnitude-duration representation of the experimental flow events (dots) and critical curves (Equation 3, for various values of drag coefficients).

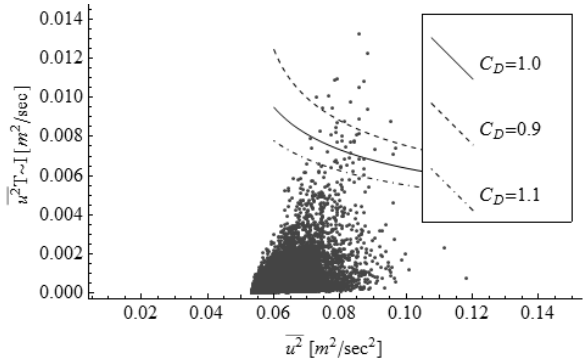

Figure 8. Representation of impulse content of flow events (dots) and critical curves (Equation 3, for various values of drag coefficients).

The variation of the theoretically predicted critical level for different values of the drag coefficient is shown in Figures 7 & 8. The greater the cumulative impulse is the higher the gain of particle's momentum or equivalently the angular velocity obtained. Thus data points with high impulse content (Figure 8) correspond to those with high mean angular velocity (Figure 4c).

4.4 *Trajectory analysis*

Coupled measurements of the local flow field and onset of particle's motion at near threshold conditions, can only be accurately obtained using non-intrusive equipment, due to the high sensitivity of bedload transport to small changes of the shear stress (Paintal 1971b). Methods such as high speed cinematography have been employed in addition to image analysis techniques (Sechet & Le Guennec 1999, Papanicolaou et al. 1999, Böhm et al. 2006).

Here detailed trajectories of particle movement are acquired using the aforementioned He-Ne laser and photodetector. These measurements are synchronous to Laser doppler velocimetry (LDV) measurements of the instantaneous velocity upstream the particle (Figure 9). The normalized He-Ne measurements (Figure 10) of angular displacement ($\Delta\theta/\Delta\theta_{max}$) are highly accurate (background noise level of background noise level of about $\pm$ 1.4%) by minimization of the ambient light interfering with the setup. This allows for a precise determination of the instance (first vertical dashed line, Figures 9 & 10) and conditions for particle entrainment.

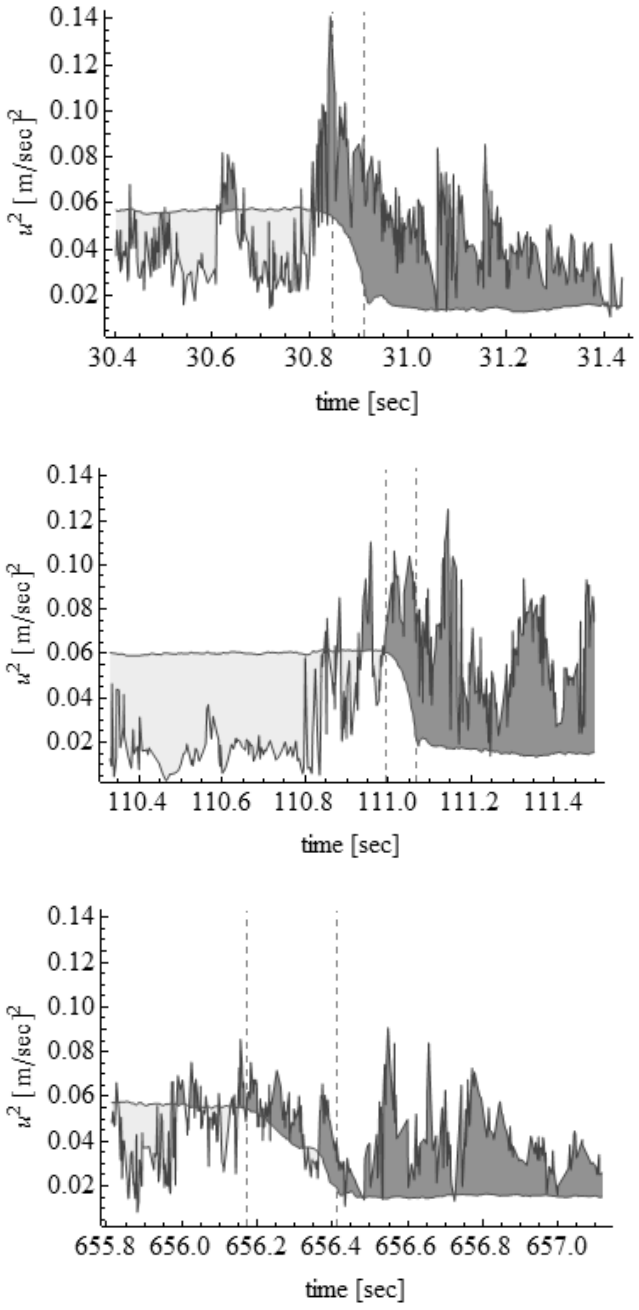

Figure 9. Hydrodynamic forcing and critical force levels for typical entrainment events. Shaded area corresponds to cases of positive (orange) to negative (yellow) change in particle momentum per unit mass (impulse).

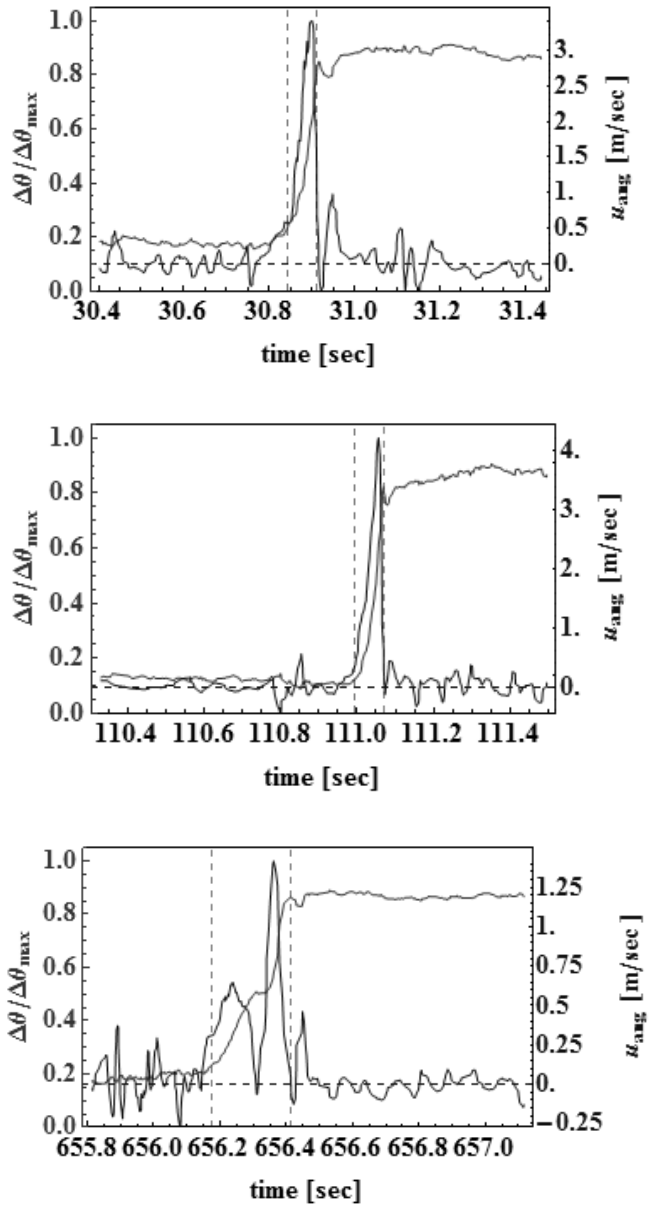

Figure 10. Characteristic dynamics of typical particle trajectories (corresponding to Figure 9) using normalized angular displacements and angular velocities.

The time required for maximum dislodgement can be deduced from the difference of the time instances for cessation (second dashed vertical line, Figures 9 & 10) and commencement of motion. The hydrodynamic forcing history on the test grain (Figure 9a) is shown along with the varying level of critical forcing due to gravity. The changes on the critical resistance level are computed from the displacement measurements implementing the momentum balance equations. When the critical level is below the hydrodynamic forcing (u^2), the momentum transfer to the grain is positive, having the potential for particle dislodgement. As confirmed from Figure 9a, small impulses (at instance of 30.6 sec) are not capable of displacing the grain. On the contrary, a series or a combination of sufficiently persisting, high magnitude impulses may result in grain entrainment (Figure 9b and c). For insufficient impulse durations the particle can only perform a twitching or pivoting motion, eventually falling back to its pocket under the influence of gravity. Figure 9b relates to the case of highest mean angular velocity and consecutively impulse while Figure 9c is linked to the flow event of the lowest magnitude (closer to threshold).

The typical particle trajectories and angular velocities (u_{ang}) corresponding to each case are shown in Figure 10, illustrating the dynamics of entrainment. Figures 10a & 10b are demonstrative of a single impulse and sequence of impulses respectively. Due to the high magnitude and long duration of the offered impulses, the momentum imparted is greater. The accelerating phase has practically the same duration as the time for entrainment, which explains the relatively increased angular velocities at the topmost position (more than 3.3 and 4.1 m/sec respectively).

In Figure 10c, a decelerating phase is discerned due to the reduction of hydrodynamic forcing below critical (Figure 9c). The motion of the particle stops (u_{ang}=0) when half of the displacement is completed. Then a secondary impulse arrives to push it further downstream. Note that this impulse on its own has significantly smaller magnitude compared to the primary ones (25 to 50%), but it is rendered more effective after the particle is brought to a position with reduced resisting forces. Again as observed in Figure 4c, the longer the duration for entrainment the less energetic and closer to threshold the dislodgement will be. Those cases can be modeled based on the suggested criterion.

5 CONCLUSIONS

The impulse model is extended to include the cases of multiple impulses having a combined effect on particle dislodgement. The new model is based on the assumption that the effect of secondary impulses with regard to the particle's response is increased after the primary impulses have set the sphere in motion. Statistical analysis of the entrainment events and characteristic variables is performed. Reliability theory is employed in defining the probability a particle will be entrained in a given duration. The proposed model is further validated with appropriately designed experiments utilizing non-intrusive equipment. The experimental results are reproduced from the theoretical predictions, implying that the criterion is promising. The trajectories of typical entrainment events are analyzed, offering a greater understanding on the relation between the applied forcing and corresponding particle's response.

ACKNOWLEDGEMENT

The support of the National Science Foundation (EAR-0439663 and EAR-0738759) and Army Research Office is gratefully acknowledged.

REFERENCES

Ancey, C., A. C. Davison, et al. (2007). "Entrainment and motion of coarse particles in a shallow water stream down a steep slope." Journal of Fluid Mechanics.

Böhm, T., P. Frey, C. Ducottet, C. Ancey, J. Magali, J. Reboud (2006). "Two-dimensional motion of a set of particles in a free surface flow with image processing." Experiments in Fluids 41(1): 1-11.

Chin, C. O. and Y. M. Chiew (1993). "Effect of Bed Surface Structure on Spherical Particle Stability." Journal of Waterway, Port, Coastal, and Ocean Engineering 119(3): 231-242.

Coleman, N. (1967). A theoretical and experimental study of drag and lift forces acting on a sphere resting on a hypothetical streambed. paper presented at 12th Congress of the International Association for Hydraulic Research, Fort Collins, Colo.

Diplas, P., Dancey, C. L., Celik, A. O., Valyrakis, M., Greer, K., Akar, T. 2008. The role of impulse on the initiation of particle movement under turbulent flow conditions. Science, 322, 717-720

Drake, T. G., Shreve, R. L., Dietrich, W. E., Whiting, P. J. & Leopold, L. B. (1988). Bedload transport of fine gravel observed by motion picture photography. Journal of Fluid Mechanics 1(192): 193-217.

Fenton, J. D. and J. E. Abbott (1977). "Initial movement of grains on a stream bed: The effect of relative protrusion." Proceedings of the Royal Society of London, Series A 352(1671): 523–537.

James, C. S. (1990). "Prediction of entrainment conditions for nonuniform, noncohesive sediments." Journal of Hydraulic Research 28(1): 25-41.

Hofland, B., J. A. Battjes, R. Booij (2005). "Measurement of Fluctuating Pressures on Coarse Bed Material." Journal of Hydraulic Engineering 131(9): 770-781.

Hofland, B. and J. Battjes (2006). "Probability Density Function of Instantaneous Drag Forces and Shear Stresses on a Bed." Journal of Hydraulic Engineering 132(11): 1169–1175.

Kaplan, E. L. and P. Meier (1958). "Nonparametric Estimation from Incomplete Observations." Journal of the American Statistical Association 53(282): 457-481.

Kirchner, J. W., Dietrich, W. E., Iseya, F., and Ikeda, H. (1990), The variability of critical shear stress, friction angle, and grain protrusion in water-worked sediments, Sedimentology 37(4), 647–672.

Komar, P. D. and Z. Li (1988). "Application of grain-pivoting and sliding analyses to selective entraiment of gravel and to flow-competence evaluations." Sedimentology 35: 681-695.

Ling, C.-H. (1995). "Criteria for incipient motion of spherical sediment particles." Journal of Hydraulic Engineering 121(6): 472-478.

McEwan I., Heald J. 2001. Discrete particle modeling of entrainment from flat uniformly sized sediment beds. Journal of Hydraulic Engineering, 127(7), 588-597.

Paintal, A. S. 1971a. A stochastic model of bed load transport. Journal of Hydraulic Research, 9(4), 527–554.

Paintal, A. S. 1971b. "Concept of Critical Shear Stress in Loose Boundary Open Channels." Journal of Hydraulic Research 9(1): 91-113.

Papanicolaou, A. N., P. Diplas, M. Balakrishnan, C.L. Dancey (1999). "Computer vision technique for tracking bed load movement." Journal of Computing in Civil Engineering 13(2): 71-79.

Papanicolaou A. N., Diplas, P., Evaggelopoulos N., Fotopoulos S. 2002. Stochastic Incipient Motion Criterion for Spheres under Various Bed Packing Conditions. Journal of Hydraulic Engineering, 128(4), 369-380.

Schmeeckle M. W., Nelson J. M. 2003. Direct numerical simulation of bedload transport using a local, dynamic boundary condition. Sedimentology, 50(2), 279-301.

Schmeeckle M. W., Nelson J. M., Shreve R. L. 2007. Forces on Stationary Particles in Near-Bed Turbulent Flows. Journal of Geophysical Research, 112, F02003.

Sechet, P. and B. Le Guennec (1999). "Bursting phenomenon and incipient motion of solid particles in bed-load transport." Journal of Hydraulic Research 37(5): 683-696.

Shvidchenko, A. B. and G. Pender (2000). "Flume study of the effect of relative depth on the incipient motion of coarse uniform sediments." Water Resources Research 36(2): 619-628.

Sumer, B. M., L. H. C. Chua, et al. (2003). "Influence of Turbulence on Bed Load Sediment Transport." Journal of Hydraulic Engineering 129(8): 585-596.

Syvitski, J. P. M., Vörösmarty, C. J., Kettner, A. J. & Green, P. 2005. Impact of humans on the flux of terrestrial sediment to the global coastal ocean. Science 308: 376-380.

Tucker, G. E., and D. N. Bradley (2009), The Trouble with Diffusion: Reassessing Hillslope Erosion Laws with a Particle-Based Model, J. Geophys. Res., doi:10.1029/2009JF001264, in press.

Valyrakis M., Diplas P., Celik A. O., Dancey C. L. 2008. Investigation of evolution of gravel river bed microforms using a simplified Discrete Particle Model, Proceedings of River Flow 2008, Ismir, Turkey, 03-05 September 2008, 10p.

Valyrakis M., Diplas, P., Dancey, C. L., Greer, K. & Celik A. O. 2010. The role of instantaneous force magnitude and duration on particle entrainment. Journal of Geophysical Research, 115, F02006, doi:10.1029/2008JF001247.

Vollmer, S., and M. G. Kleinhans (2007), Predicting incipient motion, including the effect of turbulent pressure fluctuations in the bed, Water Resources Research, 43, W05410, doi:10.1029/2006WR004919.

White, C. M. (1940), The Equilibrium of Grains on the Bed of a Stream, Proc. R. Soc. London A, 174(958), 322-338.

Wu, F.-C. and Y.-J. Chou (2003). "Rolling and Lifting Probabilities for Sediment Entrainment." Journal of Hydraulic Engineering 129(2): 110-119.

Zanke, U. C. E. (2003). "On the influence of turbulence on the initiation of sediment motion." International Journal of Sediment Research 18(1): 17-31.

Williams, J. J. 1990. Video observations of marine gravel transport. Geo-Marine Letters 10(3): 157-164.

Yeganeh-Bakhtiary, A., Shabani, B., Gotoh, H. 2009. A three dimensional distinct element model for bed-load transport. Journal of Hydraulic Research, 47(2), 203-212.